



Observed and estimated atmospheric thermodynamic instability using radiosonde observations over the city of Rio de Janeiro, Brazil

Fabricio Polifke da Silva^{1,3} · Otto Corrêa Rotunno Filho¹ · Maria Gertrudes Alvarez Justi da Silva² · Rafael João Sampaio^{1,3} · Gisele Dornelles Pires^{1,3} · Afonso Augusto Magalhães de Araújo⁴

Received: 4 June 2018 / Accepted: 26 July 2019 / Published online: 7 August 2019
© Springer-Verlag GmbH Austria, part of Springer Nature 2019

Abstract

Estimating critical weather conditions for the generation of storms with heavy rainfall represents one of the main challenges in the scientific community, especially in the warm season. While the use of radiosonde data is a possible option, an important limitation for achieving reliable forecasting of extreme rainfall events is undoubtedly low spatio-temporal resolution. As such, this research work endeavored to provide a special contribution by analyzing radiosonde data specifically collected for such evaluation applied to a tropical area, namely the city of Rio de Janeiro, Brazil. In that context, we applied a method recommended by previously reviewed literature consisting of replacing air temperature of a sounding probe launched in the morning (12 UTC) with forecasted values using data observed in the afternoon in order to gauge the method. Data points measured by radiosondes launched in the afternoon (between 12 and 7 pm local time) were used to evaluate the proposed method. The results showed that the atmosphere presented the highest heating rates in the atmospheric layer closest to the surface during the afternoon for diurnal clouds (DC) days. Similar behaviour was observed for the days of the South Atlantic Convergence Zone (SACZ). For days with frontal system (FS) presence, however, lower temperature values were observed in the afternoon in relation to the measured by morning soundings. Winds presented northeast and southwest components leading to the occurrence of warm and cold advection, respectively, in the analyzed region. Thermodynamic variables tended to be overestimated in relation to observed field results in most of the analyzed days.

Responsible Editor: M. Telisman Prtenjak.

Electronic supplementary material The online version of this article (<https://doi.org/10.1007/s00703-019-00688-3>) contains supplementary material, which is available to authorized users.

✉ Fabricio Polifke da Silva
fabricio@coc.ufrj.br

Otto Corrêa Rotunno Filho
otto@coc.ufrj.br

Maria Gertrudes Alvarez Justi da Silva
justi.meteoro@gmail.com

Rafael João Sampaio
joaosampaio@ufrj.br

Gisele Dornelles Pires
unigenharia@gmail.com

Afonso Augusto Magalhães de Araújo
afonsoaraujo@poli.ufrj.br

¹ Civil Engineering Program, Alberto Luiz Coimbra Institute for Postgraduate Studies and Research in Engineering

1 Introduction

Rainfall events in the state of Rio de Janeiro are driven by diurnal convection, i.e., storms that occur without any clear synoptic-scale forcing mechanisms present (Teixeira and Satyamurty 2007), the presence of the South Atlantic

COPPE, Universidade Federal Do Rio de Janeiro,
Rio de Janeiro, RJ 21945-970, Brazil

² Meteorology Laboratory, Science and Technology Center, Universidade Estadual Do Norte Fluminense Darcy Ribeiro UENF, Avenida Brenand, s.n, Imboassica, Macaé, RJ 27925-535, Brazil

³ Engineering and Society Group, Exact Sciences and Technologies School, Universidade Iguazu UNIG, Av. Abílio Augusto Távora, 2134, Jardim Nova Era, Nova Iguaçu, RJ 26275-580, Brazil

⁴ Department of Water Resources and Environment, Polytechnic School, Universidade Federal Do Rio de Janeiro UFRJ, Av. Athos da Silveira Ramos, CT, Cidade Universitária, Rio de Janeiro, RJ 21941-590, Brazil

Convergence Zone (Ferreira et al. 2004; Seluchi and Chou 2009) and frontal systems (Seluchi and Chou 2009; Dereczynski et al. 2009). The SACZ phenomenon is characterized by the persistence of a cloud band (NW–SE), which extends from the south central Amazon towards the southwest Atlantic Ocean (Satyamurti and Rao 1988; Ferreira et al. 2004). Frontal systems connected to extratropical cyclones move (within the 20°S–35°S latitude range) to the northeast in the South America continent, while diurnal clouds are generally formed mainly by surface heating and moisture convergence. Especially during the warmer season, the presence of these meteorological systems creates atmospheric conditions favourable to the occurrence of storms, rainfall and, in some cases, natural hazards such as floods and landslides (Roe et al. 2003; Barros et al. 2004; Boers et al. 2015; Oakley et al. 2017).

Local severe storms are generally related to heavy rainfall rates, and their detection still remains a daily challenge to operational forecasting and research communities (Das et al. 2008; Li et al. 2017). Deep convective clouds develop on a rather small spatial and temporal scale (in the order of 1–10 km and 1–12 pm), and consequently, their forecast requires adequate simulation of many processes acting on different spatio-temporal scales and their complex interactions in numerical weather prediction (NWP) models. Moreover, deep moist convection represents an intrinsic source of predictability uncertainty, especially because they are often formed in environments in which mesoscale and storm-scale processes play critical roles and those processes, in turn, are very sensitive to the specificities of their local environments (Kunz 2007; Davolio et al. 2009; Miglietta et al. 2016; Schumacher and Petersa 2017). Also, the parameterizations of moist processes still relies on simplifying assumptions, either for the sake of computational efficiency or due to uncertainties about microphysics processes and cloud-scale transport (Davolio et al. 2009; Coleman et al. 2010; Wyszogrodzki et al. 2013).

Over the last decades, the ability to predict the weather and simulate the climate using numerical models has strongly benefited from strides in computer technology development and greatly increased understanding of the land–ocean–atmosphere system (Lopez 2007). Despite the remarkable improvements achieved by NWP models over the last decades, as well as increased horizontal and vertical resolutions and shorter forecast times, prediction timing related to spatial location and precipitation intensity is usually not yet more timely NWP output with satisfactory accuracy (Davolio et al. 2009). Besides the expressive progress during the last years in the improvement of Earth system models (ESMs), most current models still present serious deficiencies in simulating and forecasting the convective activity, especially during the warm season, over the tropical regions of Southern Hemisphere. As a result, regarding

deep moist convection, the reliability of numerical modeling is still below expectations for early warning periods required in operational environments (Jewell and Brimelow 2009; Onderlinde and Fuelberg 2014; Silvestro et al. 2015).

As we know, an important guideline for storm forecasting is the knowledge of critical weather conditions for determining the potential of their development and the corresponding damage to society (Brooks et al. 2006; Silva et al. 2017). Therefore, estimating the possibility of deep moist convection development based on tropospheric instability analyses represents a common forecast problem for operational meteorologists, notably so in the warm season (Marinaki et al. 2006; Silva et al. 2017). Consequently, improving the knowledge and prediction of diurnal clouds, especially severe ones (Cumulonimbus), still represents a challenging task that may help to prevent or mitigate damages (Huntrieser et al. 1996; Kunz 2007).

The evaluation of atmospheric convective activity is a particularly important process due to the role that it plays in the release of latent heat, cloud development, and the associated precipitation (Tuttle and Davis 2006; Trier et al. 2010). These characteristics can be addressed through atmospheric conditions calculated by thermodynamic, dynamic, and kinematic parameters present in the atmosphere. These parameters are commonly called instability indices (or "severe weather parameters"), and their use for the diagnosis and prediction of storms can be performed in dichotomous or continuous manner (Haklander and Van Delden 2003). Thus, if the required atmospheric parameters are present at a given time of forecast, then the formation of storms and rain can be potentially expected. However, if such parameters are not present in the coming forecast hours, precipitation formation is unlikely to occur in the period (Wetzel and Matin 2001).

Severe weather parameters based on vertical temperature, humidity, and wind profiles are used to synthesize some thermodynamic and vertical shear characteristics of winds typical of convective situations. Among the latter, two categories are distinguished: (1) large accumulations of rainfall, without hail and with moderate wind; usually longer rains coming from stationary systems or from successive series of systems that have a similar trajectory; (2) great rainfall intensities, hailstorms, and strong winds. In general, convective cells discrete in nature have a well-defined path and do not produce large accumulations of rain; there is a possibility of downbursts, microbursts, and tornadoes, but each case has to be monitored closely (Silva Dias 1987; Silva Dias 2000).

Many authors (Jacovides and Yonetani 1990; Tajbakhsh et al. 2012) corroborate the conclusion that areas with high storm formation potential can be evaluated via techniques that combine temperature and moisture changes between the lower and middle atmospheric levels. Using the adiabatic parcel method, instability indices are designed to evaluate the likelihood with which an air parcel can rise through the

atmosphere. Thus, temperature differences between the parcel and its surrounding environment—a consequence of the initial parcel lifted along a pseudo-adiabatic process—are used as a quantitative and qualitative measure of the development of convective clouds (Manzato and Morgan 2003; DeRubertis 2006; Silva et al. 2017; Silva et al. 2018). According to the authors, some indices may be better at forecasting storms embedded in a large-scale system, while others may better characterize environmental conditions for isolated diurnal clouds. Nevertheless, it is always necessary to look the large-scale atmospheric conditions in the evaluation of instability indices.

Nascimento (2005) reports on a possible operational strategy for the forecast of severe storms in Brazil involving the calculation of meteorological parameters that objectively and accurately outline the favorable conditions for the development of severe convection, which can be obtained from observations of radiosonde, observational data, and mesoscale model results within a typical cycle of short-term forecasting operation (Westwater 2003; Mattioli et al. 2007; Kottayil et al. 2001). However, understanding this behavior over tropical regions is still a rather complex task to operational forecasters.

Under this framework, several thermodynamic parameters—like lifted index (LI), level of free convection (LFC), level of neutral buoyancy (LNB), convective available potential energy (CAPE), convective inhibition (CIN), K index (K), total totals (TT) index, Showalter index (S), maximum updraft speed (W_{max} or just W), among others—are used to measure atmospheric stability (Ratnam et al. 2003; Silva et al. 2017). However, some of these parameters show great dependence on diurnal heating and moisture availability near the surface, such as LI, LFC, LNB CAPE, CIN, and W (Fig. 1), which will be briefly discussed in this research. Further discussion of the thermodynamic and dynamic parameters can be found in Silva et al. (2018).

Convective available potential energy (CAPE) measures the difference between the virtual temperature of the parcel $T_{vp}(z)$ lifted from the surface and the virtual temperature of the surrounding environment $T_v(z)$ from the level of free convection (LFC) until the level of neutral buoyancy (LNB). The CAPE index is a measure of “positive area” (red region in Fig. 1) and also represents the energy and potential strength of updrafts within a thunderstorm (Bluestein 1993; Derubertis 2006). The atmosphere is potentially unstable when CAPE is greater than zero (typically above 1000 J/kg). In general, the higher the CAPE value, the more prone the atmosphere is to the development of storms in the presence of dynamic forcing (Blanchard 1998; Silva et al. 2016). The formal definition of the index is given by the following:

$$CAPE = g \int_{LFC}^{LNB} \frac{T_{vp}(z) - T_v(z)}{T_v(z)} dz.$$

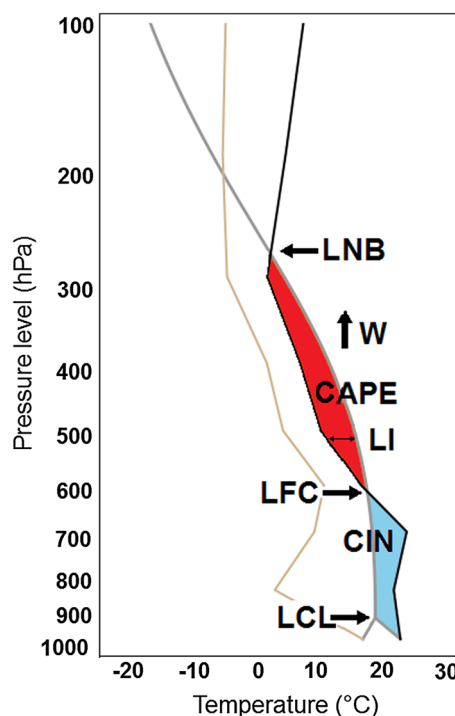


Fig. 1 Theoretical sounding and thermodynamic parameters obtained

On the opposite side of CAPE index, convective inhibition (CIN) represents the amount of work necessary to raise an air parcel from the surface (SFC) through a warmer atmospheric layer and allow this parcel to ascend until arrival at the LFC. Graphically, it is a “negative area” (blue region in Fig. 1) in the Skew T log P diagram. CIN can be calculated in a manner similar to CAPE, and is given by the following:

$$CIN = g \int_{SFC}^{LFC} \frac{T_{vp}(z) - T_v(z)}{T_v(z)} dz.$$

It is necessary to attempt not only to obtain the absolute value of CAPE, but also the vertical distribution of this energy (Silva et al. 2016, 2017), a purpose for which other single-level indices associated with the concept of buoyancy could become quite useful. One such is the Lifted index (LI), which expresses the temperature difference between a lifted parcel ($T_{vp_{500}}$) and environmental air ($T_{v_{500}}$) at 500 hPa (Galway 1956). Negative values are found for LI when the lifted parcel is warmer than its surrounding air. High-CAPE values accompanied by strongly negative LI (generally below $-5\text{ }^\circ\text{C}$) characterize a “broad positive area” in the thermodynamic diagram, which characterizes an atmospheric environment favorable to convective development and intense vertical accelerations (Foss 2011; Silva et al. 2017). LI is defined as follows:

$$LI = T_{v_{500}} - T_{v_{p500}}.$$

In high-CAPE scenarios, intense vertical acceleration (W_{\max}) values could be expected during convective activity. It is possible to estimate the maximum updraft speed W_{\max} that an air parcel may reach in a thunderstorm by calculating the square root of CAPE results (Weisman and Klemp 1982; Kirkpatrick et al. 2009). In general, the formula is given by the following:

$$W_{\max} = \sqrt{2 \times \text{CAPE}}.$$

For example, a CAPE range of 1000–2500 J/kg leads to a W_{\max} range of approximately 45–70 m/s. However, these results are not observed in nature (Holton et al. 2002). W_{\max} generally presents lower values due to the negative contributions to convective movement which can result from mass loading to condensate in updrafts and entrainment of environmental air (Kirkpatrick et al. 2009). The combination of these factors can significantly reduce rising vertical velocities (Holton et al. 2002).

The main advantages of radiosonde data are the excellent vertical resolution and good quality and simultaneous presence of temperature, wind, humidity, and pressure measurements, which are quite useful for nowcasting, and critical to determine the internal structure of severe storms and predict convection as interpreted in combination with other triggering and/or lifting mechanisms, especially in tropical regions (Silva Dias 2000; Gottlieb 2009). The greatest advantage of radiosonde data is the capability of characterizing local instability and the preconvective environment. However, one of its main limitations is their low temporal resolution in Brazil, with stations making observations only at 0000 UTC and 1200 UTC, and in some cases only once per day (Nascimento 2005; Silva et al. 2017).

As described by Silva et al. (2017), the Water Resources and Environmental Studies Laboratory (LABH2O) of the Civil Engineering Program at the Alberto Luiz Coimbra Institute for Graduate Studies and Research in Engineering—COPPE/Federal University of Rio de Janeiro (UFRJ), aiming to evaluate the preconvective and unstable atmospheric environment associated with storms and rainfall development, acquired a set of Vaisala (<https://www.vaisala.com>) radiosondes to address unexplored issues envisaging to consolidate tools and useful information for meteorologists working in an operational weather forecasting system, especially for predicting precipitation events originated by storms from diurnal convection. This line of investigation has been carried out mainly with the purpose of characterizing locally dominant mesoscale and synoptic environmental conditions favoring the formation of these storms using radiosonde data (Fawbush et al. 1953; Miller 1972; Tajbakhsh et al. 2012).

2 Methodology and data set

The primary data source for this study consisted of the measurements acquired by means of daily radiosondes launched at Galeão airport and made available by the Wyoming University database (<https://weather.uwyo.edu/upperair/sounding.html>). Since there were only two available soundings with a 12-h temporal resolution (00 UTC and 12 UTC) from which to acquire observations, operational forecasters do not have information to evaluate the thermodynamic profile in the warmer period of the day, around 13–15 h (UTC-3) local time, and it is not possible to investigate the evolution of preconvective atmospheric instability (Wagner et al. 2008; WMO 2018). Thus, when a rainfall forecast is issued for the metropolitan area of Rio de Janeiro (MARJ), additional radiosondes were launched during the afternoon to evaluate local instability (Silva et al. 2017). Figure 2 shows the sites from which the radiosondes were launched: one from Galeão airport (Ilha do Governador neighborhood) and another from the UFRJ campus in Ilha do Fundão (the two launch sites are 4.85 km apart).

As discussed by many authors, the NWP model forecasts are inherently affected by imperfect initial and boundary conditions, especially over tropical regions, numerical approximations of the dynamical equations (e.g., truncation errors), and simplifications of the complex storm-scale processes and parameters that are not easily observed (Coleman et al. 2010; Jones and Carvalho 2013; Wyszogrodzki et al. 2013; Gulizia and Camilloni 2014; Figueroa et al. 2016). As a result, investigating the atmospheric vertical profile using simple techniques, as proposed by Hart et al. (1998), can be used as an alternative to characterize the atmospheric potential to develop deep moist convection. Hart et al. (1998) propose to replace the temperature of a sounding launched in the morning with the values forecasted or observed in the afternoon to estimate thermodynamic potential. Its major use would be in morning soundings, namely by replacing the temperature of the air with another one, derived from surface observations, subjective prediction, or a numerical model forecasting, for instance (Fig. 3).

Assuming that the middle and high troposphere will not undergo significant changes, i.e., there will be no passage of a cold front or presence of other phenomena at a synoptic or larger scale, it is possible to estimate CAPE in the afternoon, when heating is higher. Thus, atmospheric environment related to the formation of diurnal clouds can be evaluated using the sounding values modified to accommodate surface condition data (Azevedo 2009). Complementing the method proposed by Hart et al. (1998), in addition to replacing the air temperature (T), replacements

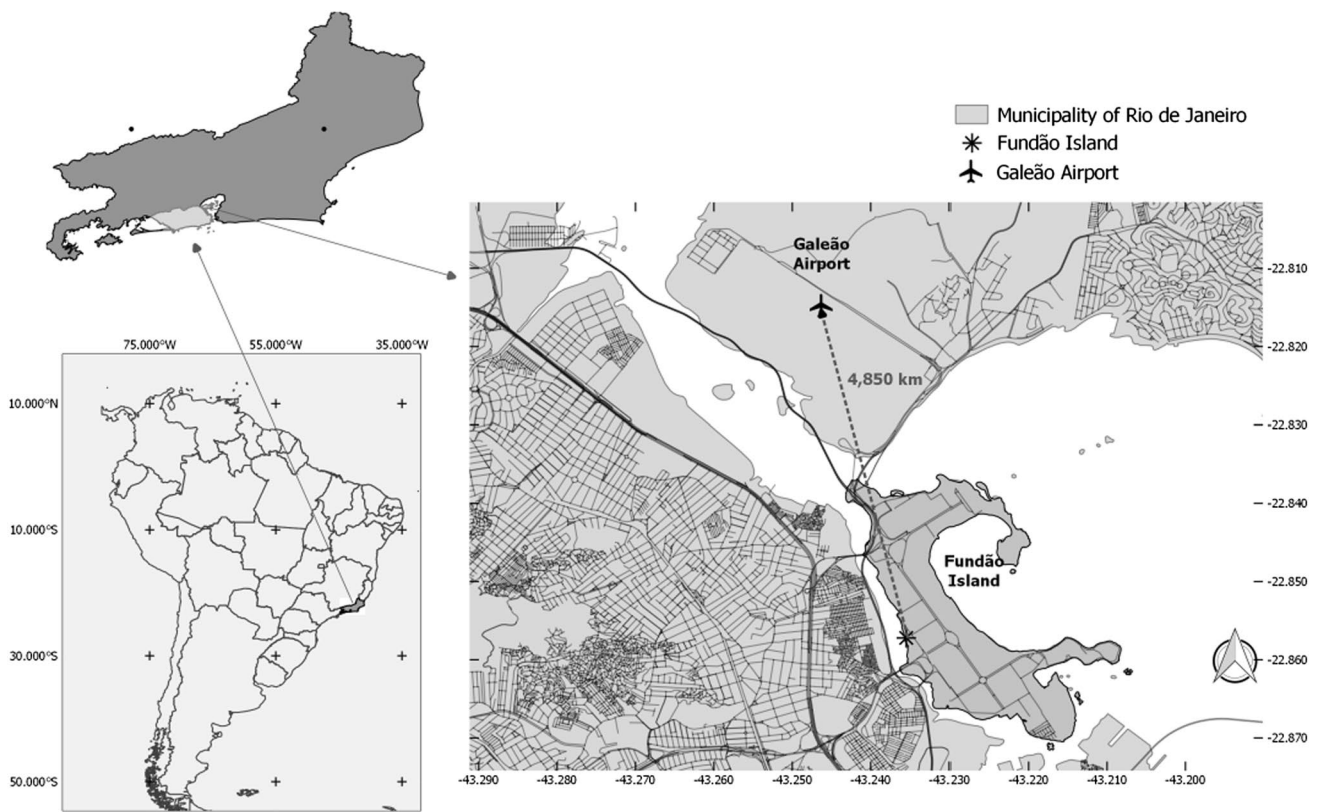


Fig. 2 Aerial view of the area of interest in the city of Rio de Janeiro, encompassing the two launch sites at Galeão airport and at the UFRJ campus located in Ilha do Fundão (Fundão Island)

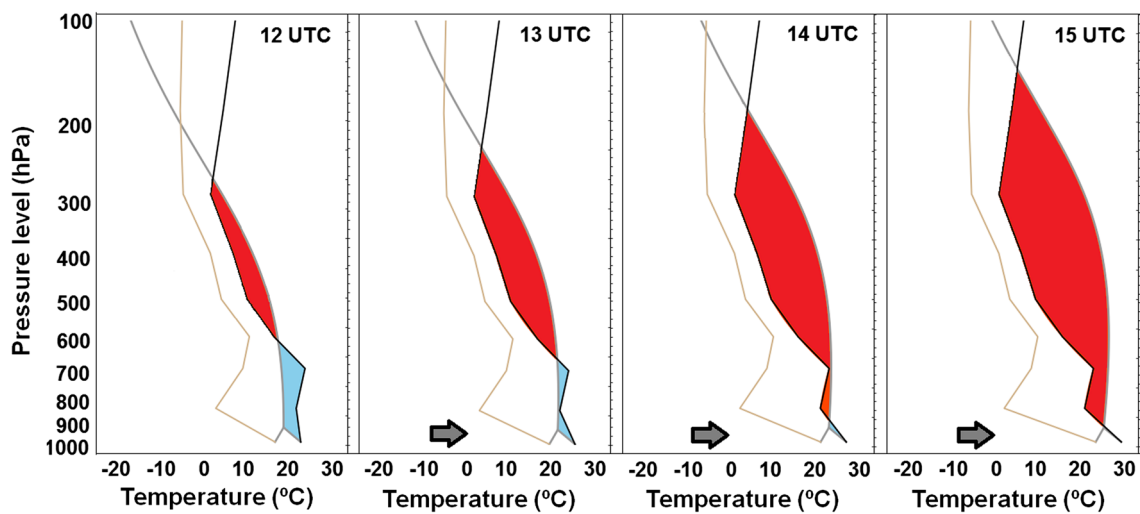


Fig. 3 Evaluation of the thermodynamic profile per the methodology proposed by Hart et al. (1998). As we modify surface data, it is possible to see an increase in CAPE (red area) and a decrease of CIN (blue area) in response to daytime heating

are carried out using dew point temperature (T_d) for measured or forecasted temperatures at the same instant of T . This additional replacement could result in a smaller error and values closer to real ones, since initial parcel

moisture has significant influence in the value of CAPE (Weisman and Klemp 1986).

The lift parcel to be used for thermodynamic profile evaluation can be chosen using three alternatives: (1)

surface-based (SB); (2) most unstable (MU) in the lower atmosphere; and (3) a mixed-layer (ML) of some predetermined atmospheric depth (McCaul and Cohen 2002). The SB parcel alternative uses surface air and dewpoint temperatures to characterize the parcel's ascent path. The MU parcel will generally produce the largest buoyancy estimations among the three lifted parcel alternatives (Schumacher and Peters 2017). The ML parcel choice is used lifting a parcel constituting a well-mixed layer of constant potential temperature and mixing ratio (Pardo 2009; Púčik et al. 2015). In this research, we have chosen the SB parcel method for the computation of thermodynamic indices due to the limitations of the Hart et al. (1998) methodology, i.e., variations in air and dewpoint surface temperature after the morning soundings for the forecasted (or later observation) values. Therefore, if this initial surface-based (SB) parcel has a large error margin, it would then be propagated to other parameters analyzed (Manzato 2008). On the other hand, it can offer a better representation of thermodynamic instability, cumulus cloud base, and severe storms (Wilde et al. 1985; Markowski et al. 2002; Gensini et al. 2014).

In light of the above, this study endeavored to intercompare the behavior of thermodynamic variables (such as CAPE, CIN, LFC, LNB, LI, and W_{\max}) obtained from the results with radiosondes launched in the afternoon and the results using the methodology proposed by Hart et al. (1998). The main objective of this research is not to specifically evaluate the behavior of thermodynamic conditions which favored the formation of thunderstorms and rainfall, but rather to evaluate the performance of the estimated thermodynamic variable results using the method proposed by Dowsell III (1987), i.e., estimated variables were compared with those actually observed using the surface-based (SB) lift. Finally, this work also endeavored to evaluate and create a relationship between estimated and observed variables to support systematic methods to diagnose and forecast the atmospheric potential to produce deep moist convection phenomena that can be of great aid to forecasters, warning systems, and civil defense personnel (Tajbakhsh et al. 2012; Silva et al. 2016, 2017).

3 Results

When there was a rain forecast for the Metropolitan Area of Rio de Janeiro (MARJ), radiosondes were launched in the afternoon with a focus on characterizing atmospheric conditions during the warm and rainy season (comprising the months from October to March) over the state of Rio de Janeiro. This radiosonde experiment occurred between November 2016 and March 2018. Pursuing the established objective, 30 days of experiment were conducted with

radiosonde launches outside the default times (00 UTC and 12 UTC).

After the experiments were carried out, the meteorological systems were characterized using meteorological weather charts prepared and provided by Brazilian Institute for Space Research (<https://www.inpe.br/>), the Brazilian Navy Meteorological Center (<https://www.marinha.mil.br/dhn/>), national weather and climate centers in Brazil, and radar imagery from the Alerta Rio system (<https://alertario.rio.rj.gov.br/>). Through this survey, it was found that the occurrence of diurnal clouds (DC—Fig. 1S) favored 80% of the events, 13% were related to Frontal Systems (FS—Fig. 2S), and 7% to the South Atlantic Convergence Zone (SACZ—Fig. 3S). For the initial discussion, we choose three days in which each individual class of meteorological systems (DC, FS and SACZ) was found over Rio de Janeiro (Table 1S) to conduct the intercomparative analysis. The chosen days were January 03, 2018 (FS), February 22, 2018 (SACZ), and March 02, 2018 (DC). These 3 days were chosen for having had the same amount of radiosondes launched during the afternoon (four) and the same time of launch, namely 12 pm, 2 pm, 4 pm, and 6 pm (four radiosondes) local time. The number of radiosondes launched was not the same in all days of the experiments due to local atmospheric characteristics, such as rainfall occurrence, strong winds, and lightning.

Following the methodology proposed by Hart et al. (1998) to compare the thermodynamic variation of the atmosphere between morning and afternoon soundings, we plotted on a single diagram the results of the morning sounding (12 UTC at Galeão) and afternoon soundings (launched at Fundão Island). The SkewT/LogP diagrams were built using the SkewT 1.1.0 Python software package (<https://pypi.python.org/pypi/SkewT>). For morning (afternoon) soundings, air temperature data are represented by a black (red) line and dewpoint temperature is represented by a blue (green) line. The CAPE values obtained using the radiosonde profile observed in the morning, modified according to surface conditions in the afternoon (CAPE_{est}), is represented by the area in gray. The CAPE values obtained using the afternoon radiosondes (CAPE_{real}) are in pink for the DC day, green for the SACZ day, and cyan for the FS day. CIN is represented in yellow for the morning radiosonde (CIN_{est}) and in orange for the afternoon sounding (CIN_{real}).

3.1 Intercomparative assessment

For the 3 days chosen with each class of meteorological systems (Figs. 4, 5, and 6), it is possible to observe a small rate of temperature variation (decrease) throughout the atmosphere, a behavior resulting from the proximity of the case study region to the Atlantic Ocean. In general, the soundings on these regions tend to exhibit less temperature variations in comparison with regions further inside the continent (Holton

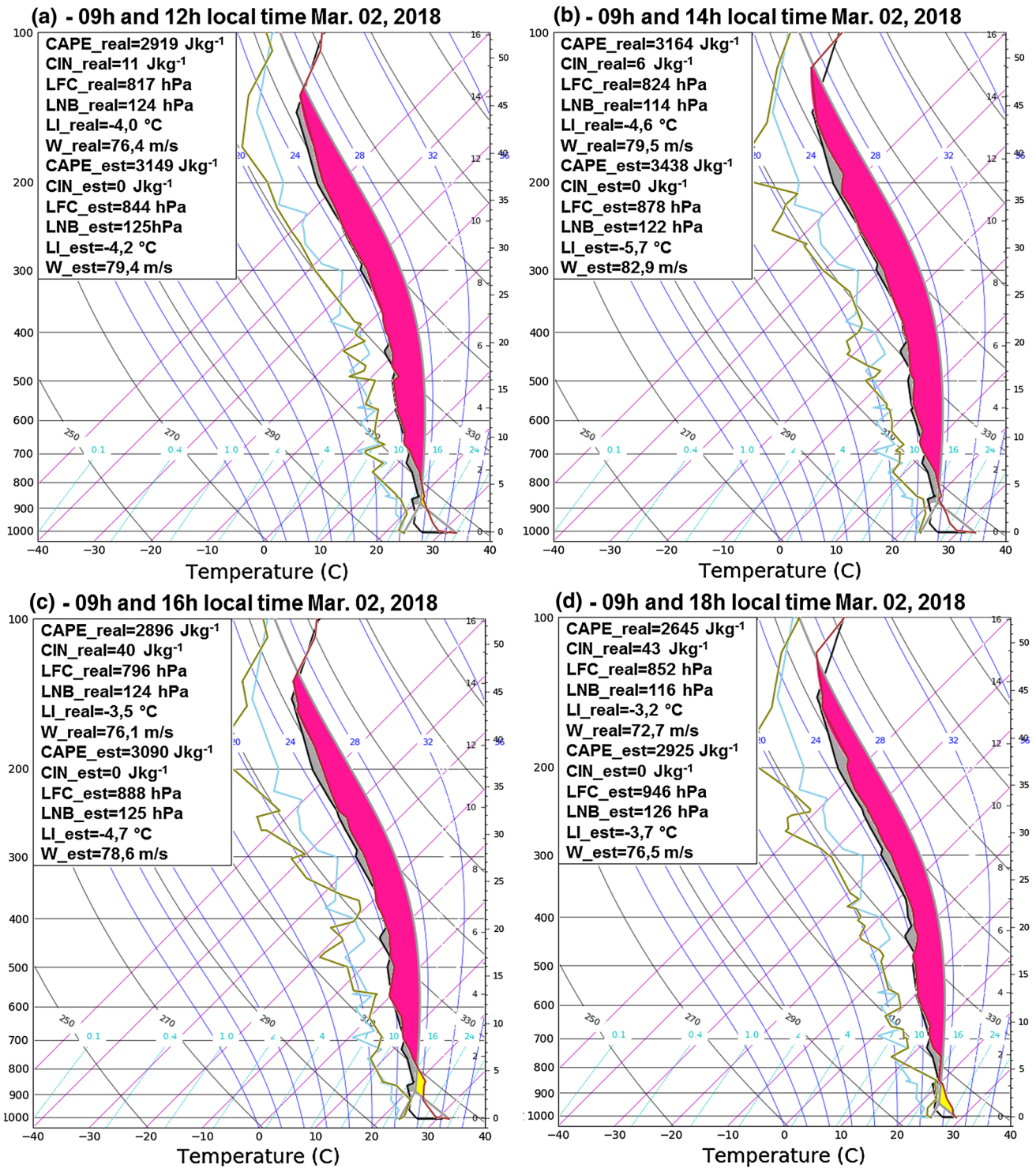


Fig. 4 Composite SkewT/LogP diagram using Galeão/RJ data (black line for air temperature and blue line for dewpoint temperature) and UFRJ/RJ data (red line for air temperature and green line for dewpoint temperature) on March 02, 2018. The Galeão/RJ sounding was measured at 12 UTC (9 am local time). The method proposed by Hart et al. (1998) was used for each sounding launched at UFRJ: **a** 12 pm

local time (3 pm UTC); **b** 2 pm local time (5 pm UTC); **c** 4 pm local time (7 pm UTC); and **d** 6 pm local time (9 pm UTC). The result for estimated CAPE (CAPE_est) corresponds to the gray area and actual CAPE (CAPE_real) corresponds to the pink area. Actual CIN (CIN_real) corresponds to the yellow area and estimated CIN (CIN_est) corresponds to the orange area

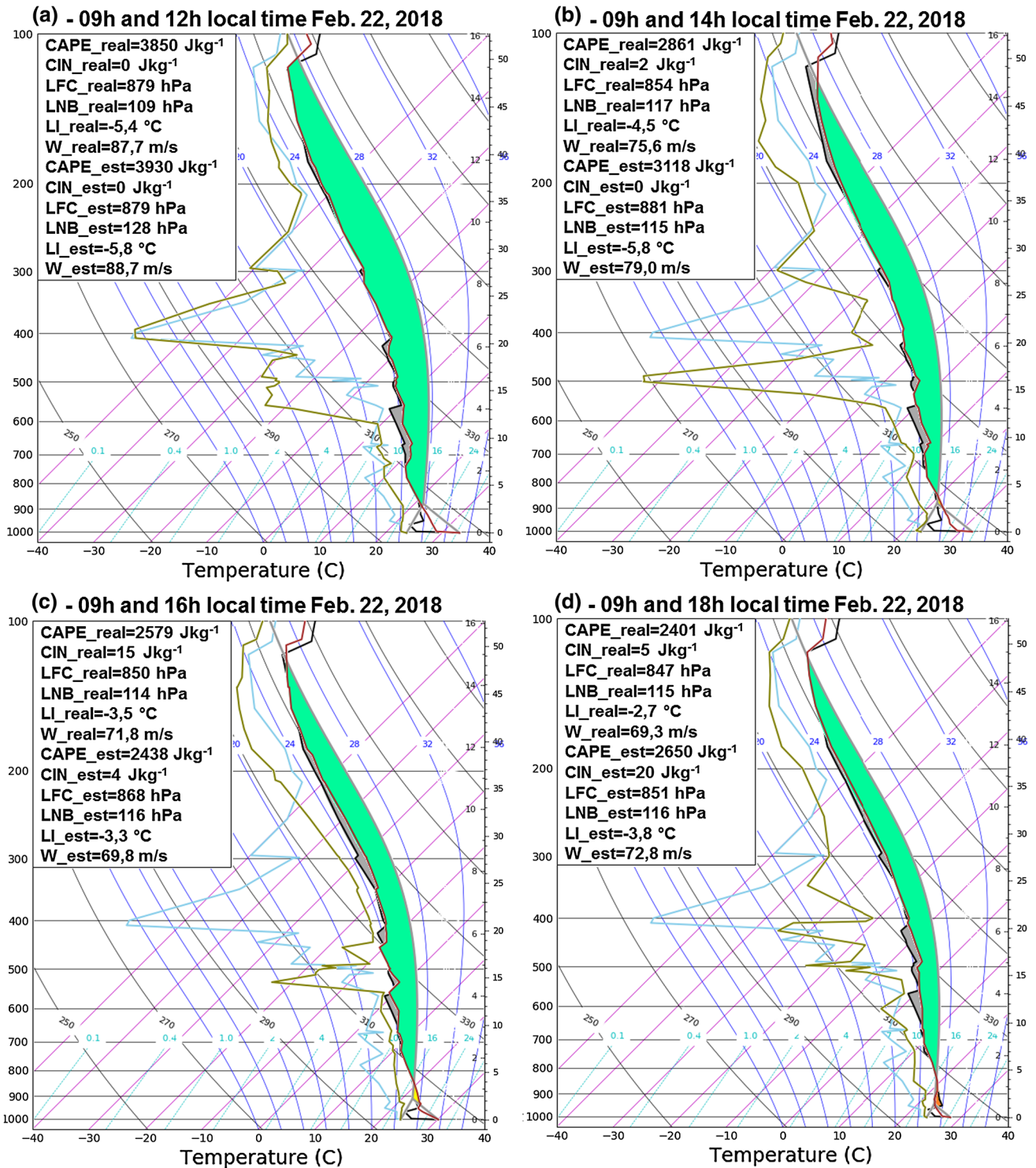


Fig. 5 Composite SkewT/LogP diagram using Galeão/RJ data (black line for air temperature and blue line for dewpoint temperature) and UFRJ/RJ data (red line for air temperature and green for dewpoint temperature) on February 22, 2018. The Galeão/RJ soundings were measured at 12 UTC (9 am local time). The method proposed by Hart et al. (1998) was used for each sounding launched at UFRJ: **a** 12 pm

local time (15 UTC); **b** 3 pm local time (17 UTC); **c** 16 h local time (19 UTC); and **d** 6 pm local time (21 UTC). The result for estimated CAPE (CAPE_est) corresponds to the gray area and actual CAPE (CAPE_real) corresponds to the green area. Real CIN (CIN_real) corresponds to the yellow area and estimated CIN (CIN_est) corresponds to the orange area

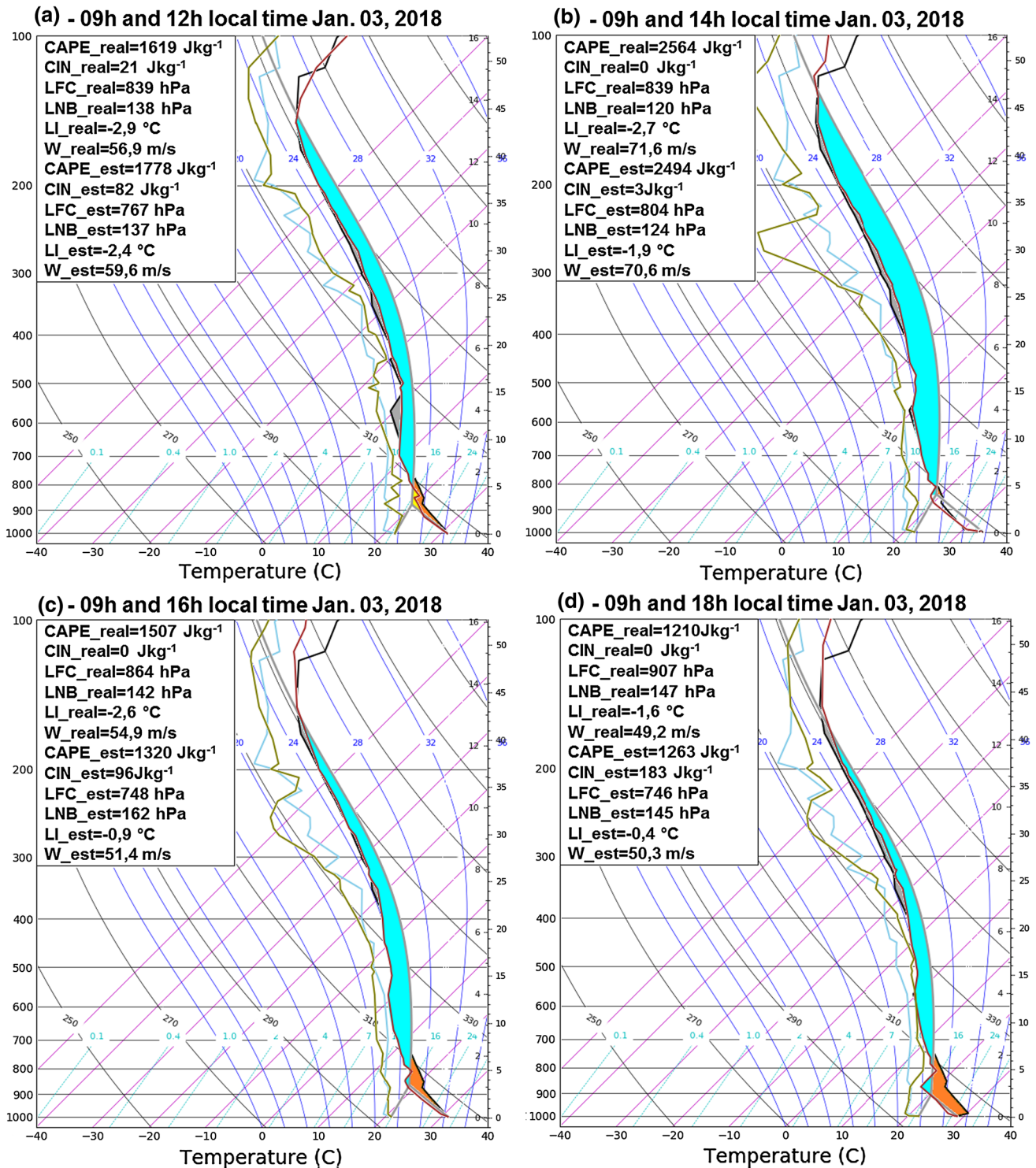


Fig. 6 Composite SkewT/LogP diagram using Galeão/RJ data (black line for air temperature and blue line for dewpoint temperature) and UFRJ/RJ data (red line for air temperature and green for dewpoint temperature) on January 03, 2018. The Galeão/RJ sounding was measured at 12 UTC (9 am local time). The method proposed by Hart et al. (1998) was used for each sounding launched at UFRJ: **a** 12 pm

local time (15 UTC); **b** 2 pm local time (17 UTC); **c** 4 pm local time (19 UTC); and **d** 6 pm local time (21 UTC). The result for estimated CAPE (CAPE_est) corresponds to the gray area and actual CAPE (CAPE_real) corresponds to the cyan area. Real CIN (CIN_real) corresponds to the yellow area and estimated CIN (CIN_est) corresponds to the orange area

et al. 2002). Small changes in the temperature profile were observed between the afternoon and morning soundings for the DC day (Fig. 4). It is also possible that the atmosphere was warmer in relation to the morning sounding, as seen by the small shift of the red line (afternoon profiles) to the right as compared to the black line (morning profile) on the diagrams (Seidel et al. 2005; Balling and Cerveny 2003). Thus, there was a smaller area of energy [difference between observed CAPE (pink) and estimated CAPE (gray)] for an air parcel rising in the atmosphere with the same values of air temperature and dewpoint temperature. Similar behaviors can be found for the other parameters.

For the FS day (Fig. 5), however, unlike what was observed on the DC diagrams, it was not possible to observe a similar tendency of changes between actual CAPE (cyan) and estimated CAPE (gray) and the other thermodynamic parameters. For example, along the 2 pm and 4 pm local time soundings (Fig. 5b and c), it was found that CAPE_est had lower values in comparison with CAPE_real, while the other soundings (Fig. 5a and d) presented the opposite behavior. The lower CAPE values observed in the FS day indicate the results of cooling and drying of the atmospheric layer associated with the cold front passage (Dourado and Oliveira 2001). For this case, we did not observe a consistent relationship between estimated CIN (CIN_est) and observed CIN (CIN_real).

For the SACZ soundings (Fig. 6), it is possible to find a similar profile of vertical variations to that observed on the DC day (Fig. 4) and FS day (Fig. 5) diagrams. A similar vertical profile is depicted for the FS day (Fig. 5), with afternoon temperatures (red line) showing a small shift to the left (cooling) compared to morning temperatures (black line) under 700 hPa. Above this level, temperature changes presented a similar trend to that observed in the DC soundings (Fig. 4). Similar to FS soundings, no similar trend was observed between actual CAPE (green) and estimated CAPE (gray) or with respect to the other variables for the SACZ day. For example, the estimated parameters for the 12 pm (Fig. 6a), 2 pm (Fig. 6b), and 8 pm (Fig. 6d) soundings presented more energy into the atmosphere, which was not observed for the 4 pm sounding (Fig. 6c).

3.2 Vertical temperature and mixing ratio changes

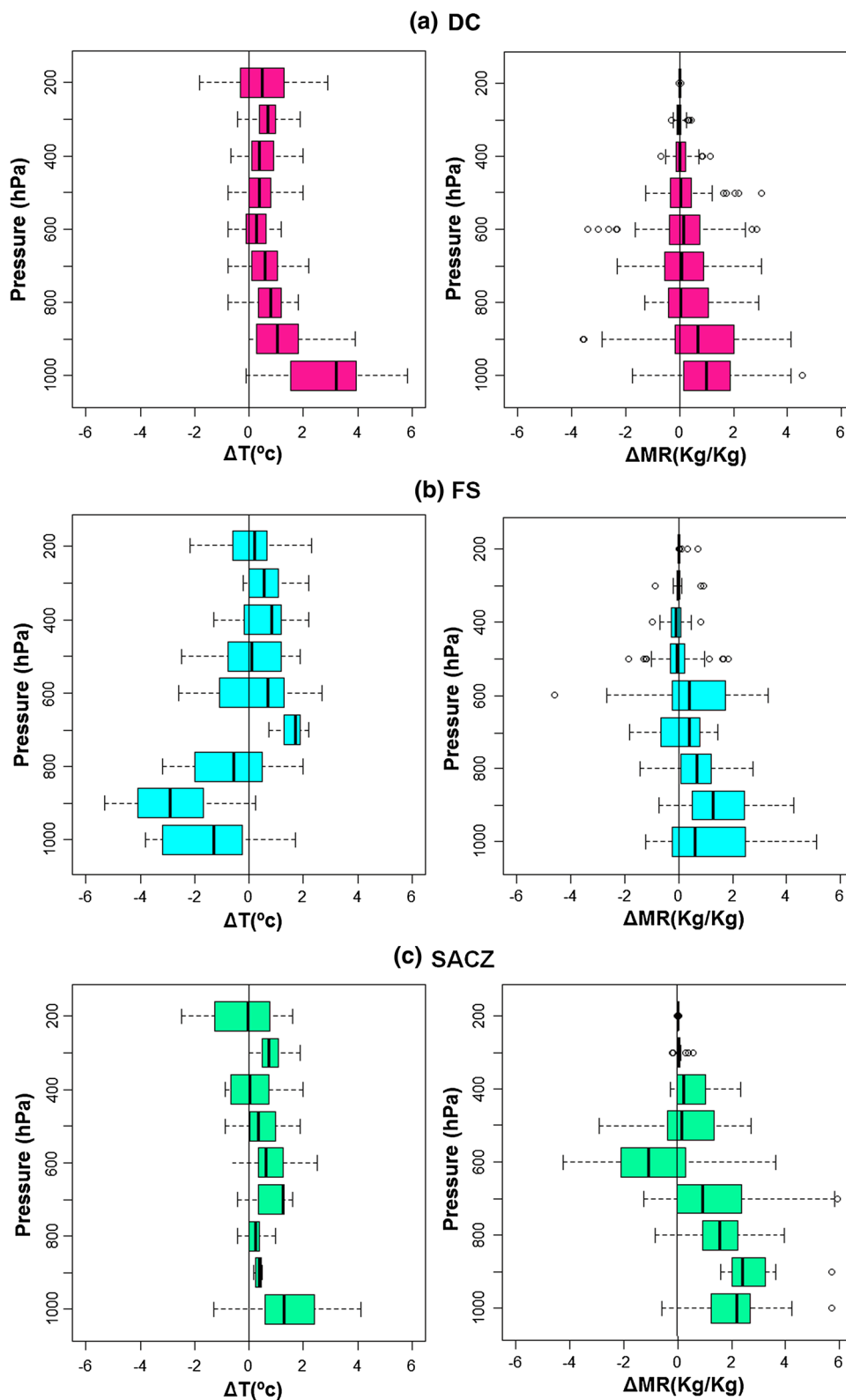
In the previous intercomparison section, we analyzed only 3 days to provide qualitative knowledge on atmospheric vertical profiles related to each meteorological class situation. In this section, all 30 days will be studied to draw quantitative conclusions regarding estimated vs. observed parameters. Figure 7 shows the vertical profile of temperature (left) and mixing ratio (right) differences between soundings released in the afternoon at Fundão Island and the soundings released in the morning at Galeão airport for DC (Fig. 7a),

FS (Fig. 7b), and SACZ (Fig. 7c) days (Table 1S). In general, the diurnal variations observed in upper air temperature for all events are mainly the result of atmospheric absorption of long-wave solar radiation, sensible and latent heat fluxes on the surface, latent heat releases within the atmosphere and temperature advection, all of which can present a variety on diurnal and semidiurnal scales (Sherwood 2000; Seidel et al. 2005).

Figure 7a (left) shows the results for all DC days analyzed. The most significant temperature and mixing ratio differences were observed in the layers closest to the surface (with positive variations up to 6 °C), which aligns with the results found by Seidel et al. (2005) and Balling and Cerveny (2003). Analyzing upper air sounding data, the authors found that the temperature changes observed were most significant in the layers closest to the surface and taper off at the upper troposphere. This is due mainly to the lower troposphere being strongly influenced by the daily cycle of surface heating and evapotranspiration due to contact with the heated ground warmed by conduction (Arya 2001; Holton et al. 2002). This behavior could also be associated with warm temperature advection by the northwest and northeast winds over the region, contributing to atmospheric destabilization in DC days (Moore et al. 1995; Schumacher and Johnson 2005). Figure 8a, in turn, reveals that the highest frequency winds during DC days present a northwestern component in the low levels of the atmosphere. A similar trend is observed in the middle (Fig. 8d) and upper (Fig. 8g) atmospheric levels. According to Teixeira and Satyamurti (2007), the northerly component winds bring moisture and warm air into southern Brazil, favoring the increased mixing ratio observed (Fig. 7a, right). This contributes to even greater enhancement of instability conditions, which, together with local topographic conditions, favors convective development over the metropolitan area of Rio de Janeiro (MARJ) (Silva et al. 2017, 2018).

For FS days (Fig. 7b, left), primarily negative temperature changes are observed in the layers between the surface and 850 hPa, while above these layers, positive and negative changes are concomitantly observed. This behavior could be a net result of daytime heating from the strong solar radiation observed during the warm season and also due to cold air advection produced by the frontal passage (Doswell and Haugland 2007; Nallapareddy et al. 2011; Silva et al. 2017). The opposite behavior is observed for the variations in the mixing ratio (Fig. 7b, right). Positive variations (and more expressive in relation to DC days) are observed between the surface and 850 hPa. This would be mainly the result of cooling temperatures and reduced volume of this atmospheric layer. Similar to DC days, minor mixing ratio variations are observed at high levels of the atmosphere. Figure 8b shows the presence of higher frequencies of the southwest wind component and lower frequencies in the

Fig. 7 Vertical temperature and mixing ratio changes between afternoon soundings (Fundão Island) and morning soundings (Galeão) for **a** DC, **b** FS, and **c** SACZ



west/northwest quadrant at the low levels of the atmosphere. In the state of Rio de Janeiro, the presence of the southwest component is one of the main characteristics of FS over the region. This component is responsible for cold advection

over the MARJ, i.e., it brings cooler air from the South (Andrade 2005). In the middle (Fig. 8e) and upper levels (Fig. 8h) of the atmosphere, northwest and west components are present, bringing air from the interior of the continent

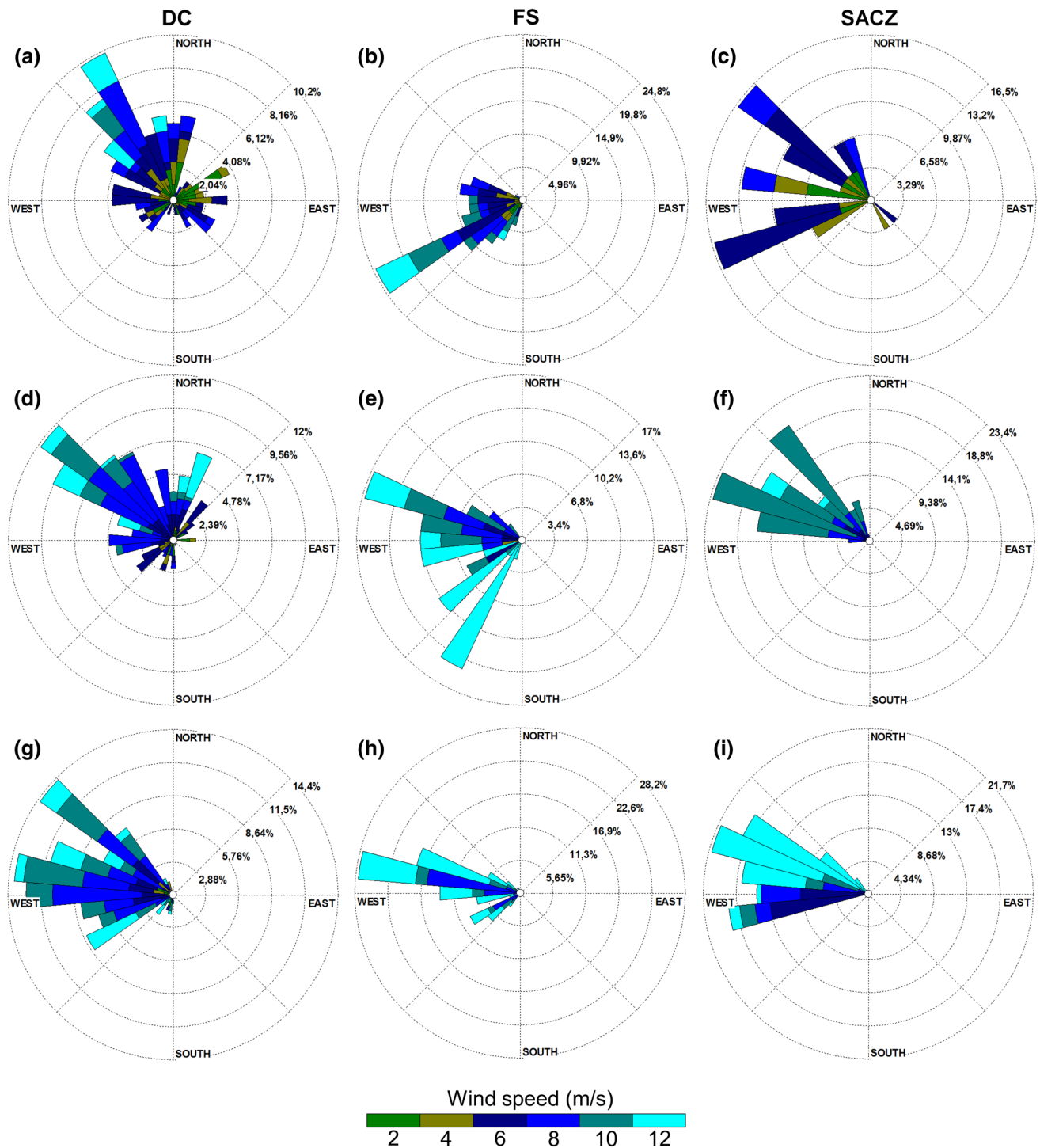


Fig. 8 Wind rose for DC, FS, and SACZ events between surface level and 850 hPa (a, b, c), 850–500 hPa (d, e, f), and 500–200 hPa (g, h, i)

(warmer) towards the MARJ and favoring the heating of the atmosphere at these levels, as could be observed in the soundings diagram (Fig. 5).

For SACZ days (Fig. 7c, left), a vertical temperature variation profile similar to that observed in DC (Fig. 7a) and FS (Fig. 7b) days was observed. However, lower rates of

variation are observed for this profile in relation to the one observed for DC and FS profiles. More expressive positive changes in the mixing ratio (Fig. 7c, right) are observed for SACZ days, which could be related to the presence of higher frequencies of the northwest component over the troposphere (Fig. 8c), a classic characteristic of the SACZ configuration

[i.e., it brings moisture from the Amazon region to Rio de Janeiro state (Satyamurti and Rao 1988; Ferreira et al. 2004; Quadro et al. 2012)]. However, a small southwest component is observed at the lower atmospheric levels in response to the general large-scale atmospheric circulation changes, which is also present in the SACZ regime over the MARJ (Andrade 2005; Nynomia 2007). The combined action of these components suggests that this phenomenon is simultaneously influenced by the presence of warm advection at low levels (from the northwest component) and cold advection above the boundary layer (from the southwest component) favoring the temperature and moisture variations observed over the region.

In addition, it was possible to identify high dependence on wind direction and speed on daytime thermal variation profiles in all the scenarios analyzed. In addition to heat transfer by the convective thermals, this analysis outlines the important role of cold and warm advectations in vertical variations of atmospheric temperature profiles (Acevedo et al. 2017). It is also possible to observe larger temperature changes in the tropopause for the three systems analyzed (Fig. 7). A second hypothesis could be the one proposed by Reid and Gage (1981), according to which the tropopause diurnal cycle appears to respond directly to surface heating deriving from solar radiation (Revathy et al. 2001). Physically, the link between surface heating and tropopause temperature variations is provided by convection of the cumulonimbus clouds of tropical regions, under which an air parcel can obtain maximum heating via release of latent heat, especially if the region is close to the shoreline, like the MARJ (Reid and Gage 1981). Despite the smaller sample for FS and SACZ days, it was verified that the trend for variations observed in these events was not similar to that observed in the DC days, highlighting the local variability of the atmosphere in the presence of these synoptic-scale meteorological systems.

3.3 Regression approach

In this section, we will describe the results of the regression approach. However, before these are introduced, we would like to emphasize that the application of this methodology and the regression adjustments found are more reliable for those days when there is no large-scale synoptic systems, such as FS and SACZ, because in the absence of these, the atmospheric profile tends not to show large changes with time above the planetary boundary layer (Azevedo 2009). We would also like to emphasize that, due to the short data set analyzed, the quantitative results might present some bias. As such, these should be interpreted carefully, as the results were obtained merely to use the observation data to understand the capacity of this methodology. On the other hand, we believe that the results can be very useful for the

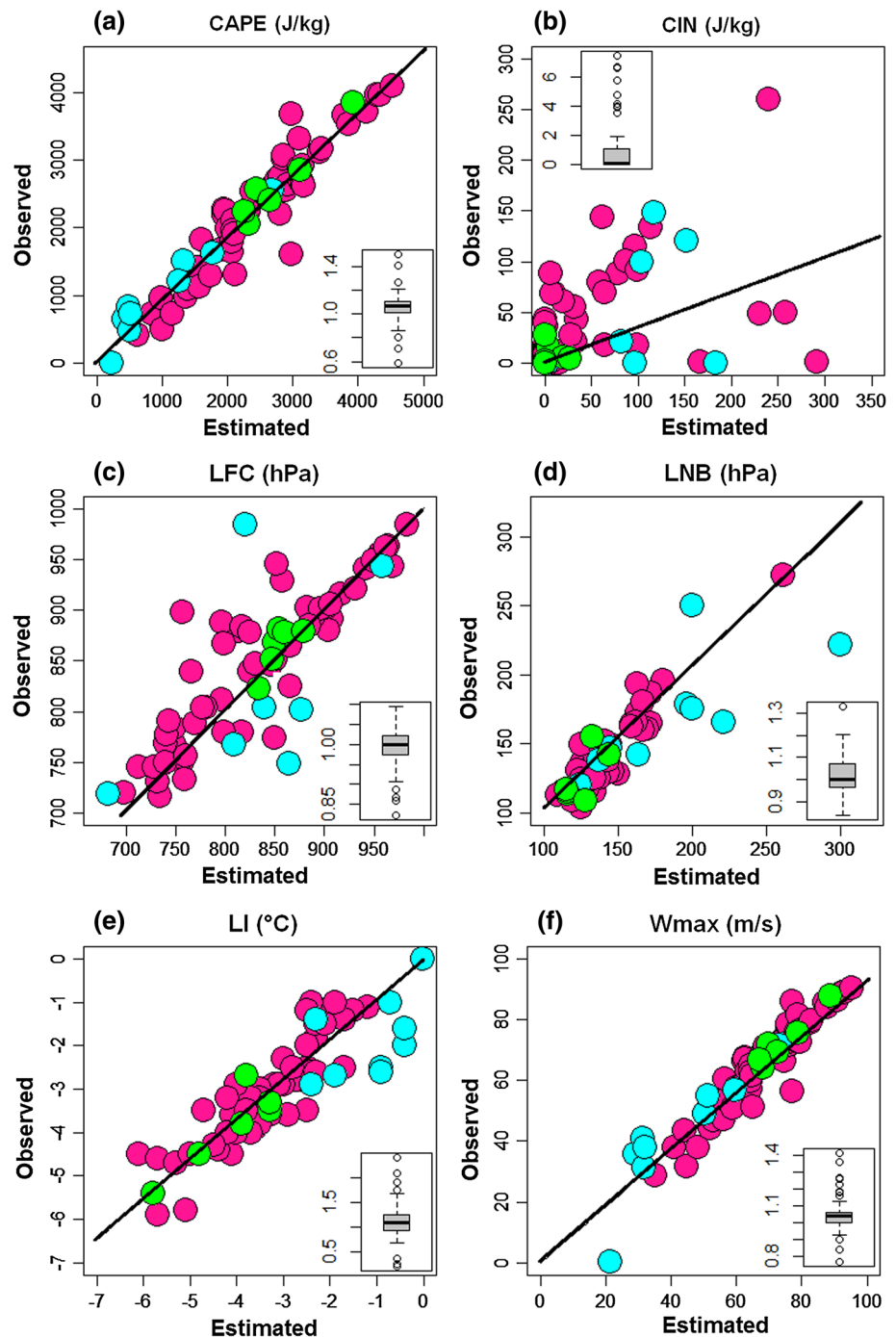
monitoring of atmospheric instability (and also for forecasts that take into account the bias between observed and forecasted air and dewpoint surface temperatures) associated with daytime heating and moisture availability, especially during the warm season over the metropolitan area of Rio de Janeiro (MARJ).

Figure 9 shows the scatter plot for all the thermodynamic variables analyzed: CAPE, CIN, LFC, LNB, LI, and W_{\max} . CAPE (Fig. 9a) and W_{\max} (Fig. 9f) were the ones which presented the higher linear trend in relation to the other parameters analyzed. This result shows that the recommendation made by Hart et al. (1998) presented greater correlation coefficients between estimated and observed behavior for these variables, with values of approximately 0.95. LFC (Fig. 9c), LNB (Fig. 9d), and LI (Fig. 9e) presented intermediary correlation coefficient values (0.79, 0.82, and 0.84, respectively). The worst discrepancies between estimated and observed results were found for the CIN parameter (Fig. 9b). This is mainly a result of a possible deficiency of the method used (Hart et al. 1998) to evaluate this variable. This behavior could be generally explained by the planetary boundary layer (PBL) warming up during the afternoon (estimated soundings using only afternoon surface temperature data could have retained the cooler PBL from the morning sounding).

The boxplot for the ratio between estimated and observed results is also showed in Fig. 9a–f. For all variables except LFC (Fig. 9c), it has been found that the average ratio is above 1.0, which characterizes that the method proposed by Dowsell III (2001) tended to overestimate the results of thermodynamic variables using morning soundings as an indicative of atmospheric instability during the afternoon. For CAPE (Fig. 9a), we have found an overestimation of CAPE_{real} in relation to CAPE_{estim} due to daytime heating of the vertical profile of the atmosphere. This heating likely causes a decrease in the area between the saturated adiabatic and the air line in the afternoon (red line) compared to morning air temperature. Consequently, the area for CAPE_{real} was smaller than that for CAPE_{estim}, causing the overestimation.

CIN (Fig. 9b) presented a greater trend for underestimation of observed CIN (CIN_{real}) vs. estimated CIN (CIN_{estim}) in comparison to the other variables. This poorer result is mainly due to the high warming observed in the PBL during the afternoon and also because the physical traits of the parameter: small changes in PBL temperature profile will yield relatively large changes in CIN. In other words, a temperature increase (decrease) of 1 °C in the PBL could yield a decrease (increase) of 50 J/kg in CIN (CAPE) results. However, 50 J/kg is more than an order of magnitude smaller than a typical afternoon CAPE value, whereas it is on the same order of magnitude for a typical CIN value (Manzato 2008). Especially on DC days with

Fig. 9 Scatter plot between the estimated and observed values of **a** CAPE, **b** CIN, **c** LFC, **d** LNB, **e** (LI), and **f** W_{\max} for DC (circles filled in pink), FS (blue), and SACZ (green) days. The black line represents the linear regression curve. The boxplot represents the ratio between estimated and observed results for each thermodynamic variable



vertical temperature changes, the vertical morning profile for PBL was colder compared to what was observed during the afternoon. Then, CIN values of zero or lower were obtained after afternoon surface conditions were applied to the morning sounding values.

For LFC (Fig. 9c), a behavior similar to CAPE and CIN is observed, although values smaller than 1.0 were found. With the drift of the red lines to the left due to daytime heating, the dry adiabatic line crossed the air temperature line at higher levels of the atmosphere compared to the

colder morning soundings, favoring an underestimation of LFC between afternoon and morning profiles. A similar pattern was observed for LNB (Fig. 9d). Our concomitant analysis of these three variables suggests that the method of Hart et al. (1998) tended to overestimate CAPE, because it considered greater vertical extension of the atmospheric layer with energy for convection, i.e., lower values of LFCs and higher ones for LNB. Similar behaviors and results are observed for LI (Fig. 9e) and W (Fig. 9f).

To find relationships between the thermodynamic results obtained from the afternoon soundings and the morning soundings using the method proposed by Hart et al. (1998) and aiming to corroborate the use of this methodology by weather forecasting and monitoring systems, we conducted a linear regression analysis of observed and estimated variables. The results can also be seen in Fig. 9a–f (black line). For example, for CAPE estimations, it was found that the estimated values can approximate real values using a simple linear relationship $CAPE_{real} = 0.927 * CAPE_{estim}$ with regression coefficient (R^2) of approximately 0.91. Thus, for the MARJ, meteorologists using the method proposed by Hart et al. (1998) could correct estimated values for CAPE toward observed CAPE in case a radiosonde was launched for the estimated time. For example, for a CAPE estimated at 4000 J/kg, the proposed regression equation would yield approximately 3708 J/kg for observed CAPE at the estimated time. The same procedures can also be repeated for the other thermodynamic variables, considering $CIN_{real} = 0.462 * CIN_{est}$ ($R^2 = 0.14$), $LI_{real} = 0.927 * LI_{est}$ ($R^2 = 0.72$), $W_{max-real} = 0.961 * W_{max-est}$ ($R^2 = 0.89$), $LFC_{real} = 1.001 * LFC_{est}$ ($R^2 = 0.58$), and $LNB_{real} = 0.975 * LNB_{est}$ ($R^2 = 0.64$), respectively.

4 Conclusions

This study reviewed the characterization of estimated atmospheric thermodynamic diurnal variability through radiosonde data for the 30 experiments conducted in the metropolitan area of Rio de Janeiro (MARJ). It was also possible to categorize the predominant meteorological systems in the period of the field experiment. It was found that the diurnal clouds (DC) accounted for 80% of the events, while frontal systems (FS) accounted for 13% and the South Atlantic Convergence Zone (SACZ) to 7% of events. However, we would also like to emphasize that, given the small size of the temporal sample (thirty days), the analyses and quantitative measurements carried out could present some bias and should be interpreted carefully. SkewT-LogP diagrams were generated for only one day for each of the three meteorological situations, i.e., March 2 (DC), February 22 (SACZ), and January 1 (FS) 2018. Through an intercomparative analysis, we found greater atmospheric instability in DC days, intermediate values for SACZ days, and the lowest values for FS days, characterizing local atmospheric variability in the presence of synoptic systems such as the SACZ and FS.

Based on the morning soundings, it was possible to use the methodology to estimate the thermodynamic variables for the warmest period of the day (afternoon) by adjusting the air temperature and dewpoint temperature surface data measured in the morning soundings. On average, we observed an increase of temperature and moisture for DC

days throughout the thermodynamic profile in relation to the morning. For FS and SACZ days, however, a different trend for vertical changes was observed throughout the atmosphere, with more expressive changes between the surface and the 850 hPa atmospheric level. These results show that the atmosphere in the presence of synoptic systems presents greater variability in relation to diurnal convection days. In the lower layers, a cooling of the troposphere was observed in comparison with morning data. Winds showed higher frequency of the northwest component during DC days and southwest and northwest components on FS days, revealing the importance of wind direction and speed on daytime thermal profile variations through warm/cold advections and moisture transport towards the Rio de Janeiro state.

Using simple linear regression, we were also able to find relationships between observed and estimated results. In most of the thermodynamic variables analyzed, it was possible to confirm that the estimated values can approximate real values using linear equations of high reliability, especially for the CAPE parameter. Thus, forecasters could easily correct the estimated values for the thermodynamic variables estimated for the afternoon period using the real data observed or forecasted by numerical models. However, the application of this methodology and the regression adjustments found that such approach is more reliable for the days when there are no large-scale synoptic systems, because in the absence of these, the atmospheric profile tends not to show large changes with time during the course of the day. We believe that the results could be very useful for the monitoring of atmospheric instability associated with daytime heating and moisture availability, especially during the warm season over the metropolitan area of Rio de Janeiro. As a possibility for future exploration, we intend to analyze the results of soundings and the predictions of numerical models to better inform decision-making by operational forecasters.

Acknowledgements The authors would like to thank the Civil Engineering Program of the Alberto Luiz Coimbra Institute of Postgraduate Studies and Research in Engineering (COPPE)—part of the Universidade Federal do Rio de Janeiro (UFRJ)—for their support, particularly offered through the Laboratory of Water Resources and Environmental Studies (LABH2O), as well as the Meteorology and Atmospheric Physics editorial board for their revisions. The authors would also like to recognize the support of the Coordenação de Aperfeiçoamento de Pessoal de Nível Superior (CAPES), which helped fund this work through CAPES Call 27/2013—Pró-Equipamentos Institucional and CAPES/MEC Call No. 03/2015—BRICS; we further thank the Conselho Nacional de Desenvolvimento Científico e Tecnológico (CNPq), which helped fund this work through CNPq Universal Call for Papers No. 14/2013—Proceeding No. 485136/2013-9 and CNPq Call No. 12/2016—Proceeding No. 306944/2016-2; the National Secretariat of Higher Education (SESu)—part of the Ministry of Education (MEC) (2010–2016) (PET CIVIL UFRJ); the Fundação de Amparo à Pesquisa do Estado do Rio de Janeiro (FAPERJ), which helped fund this work through Project FAPERJ—Pensa RiovCall 34/2014 (2014–2018)—E-26/010.002980/2014, FAPERJ No. E_12/2015 and FAPERJ nº E-22/2016; as well as the Brazilian Ministry of Science

and Technology (MCT), through its Financier of Studies and Projects (FINEP) and in particular its CT-HIDRO Fund (2005–2016), which is focused on researching rainfall–runoff and atmospheric modeling, water and energy balances, and extreme flood and drought events. This study was financed in part by the Coordenação de Aperfeiçoamento de Pessoal de Nível Superior- Brasil (CAPES)—Finance Code 001.

References

- Acevedo OC, Degrazia GA, Puhales FS, Martins LGN, Oliveira PES, Teichrieb C, Silva SM, Maroneze R, Bodmann B, Mortarini L, Cava D, Anfossi D (2017) Monitoring the micrometeorology of a coastal site next to athermal power plant from the surface to 140 m. *Bull. Am Meteorol Soc.* <https://doi.org/10.1175/BAMS-D-17-0134.1>
- Andrade KM (2005) Climatologia e comportamento dos sistemas frontais sobre a América do Sul. Dissertation, National Institute for Space Research
- Arya SP (2001) Introduction to micrometeorology, 2nd edn. Elsevier, New York
- Azevedo LHDR (2009) Avaliação de método de previsão para tempestades convectivas severas por mudança da temperatura do ar e do ponto de orvalho junto à superfície em sondagens atmosféricas. Monography, Federal University of Rio de Janeiro
- Balling RC, Cerveny RS (2003G) Vertical dimensions of seasonal trends in the diurnal temperature range across the central United States. *Geophys Res Lett* 25:25. <https://doi.org/10.1029/2003GL017776>
- Barros AP, Kim G, Williams E, Nesbitt SW (2004) Probing orographic controls in the Himalayas during the monsoon using satellite imagery. *Nat Hazard Earth Syst* 4(1):29–51
- Blanchard DO (1998) Mesoscale convective patterns of the southern high plains. *Bull Am Meteor Soc* 71:994–1005
- Bluestein HB (1993) Synoptic-dynamic meteorology in midlatitudes. Volume II: observations and theory of weather systems. New York, USA
- Boers N, Bookhagen B, Marwan N, Kurths J (2015) Spatiotemporal characteristics and synchronization of extreme rainfall in South America with focus on the Andes Mountain range. *Clim Dyn* 46:601–617. <https://doi.org/10.1007/s00382-015-2601-6>
- Brooks HE (2006) A global view of severe thunderstorms: Estimating the current distribution and possible future changes In: Preprints, Severe Local Storms Special Symposium, American Meteorological Society, Atlanta
- Coleman RF, Drake JF, McAttee MD, Belsma LO (2010) Anthropogenic moisture effects on WRF summertime surface temperature and mixing ratio forecast skill in Southern California. *Weather Forecast* 25:1522–1535
- Das S, Ashrit R, Iyengar GR, Mohandas S, Gupta MD, George JP, Rajagopal E, Dutta SK (2008) Skills of different mesoscale models over Indian region during monsoon season: Forecast errors. *J Earth Syst Sci* 117:603–620
- Davolio S, Mastrangelo D, Miglietta MM, Drofa O, Buzzi A, Malguzzi P (2009) High resolution simulations of a flash flood near Venice. *Nat Hazards Earth Syst Sci* 9:1671–1678
- Dereczynski CP, Oliveira JSD, Machado CO (2009) Climatologia da precipitação no município do Rio de Janeiro. *Rev Bras Meteorol* 24(1):24–38. <https://doi.org/10.1590/s0102-77862009000100003>
- Derubertis D (2006) Recent trends in four common stability indices derived from US radiosonde observations. *J Clim* 19:309–323
- Doswell CA, Haugland MJ (2007) A comparison of two cold fronts—effects of the planetary boundary layer on the mesoscale. *Electronic Journal of Severe Storms Meteorology.* <https://www.ejssm.org/ojs/index.php/ejssm/article/viewarticle/30/24>. Accessed 02 March 2018
- Doswell CA III (1987) The distinction between large-scale and mesoscale contribution to severe convection: a case study example. *Weather Forecast* 2:3–16
- Dourado MS, Oliveira AP (2001) Observational description of the atmospheric and oceanic boundary layers over the Atlantic Ocean. *Braz J Oceanogr.* 49:49–59
- Fawbush EJ, Miller RC (1953) A method of forecasting hailstone size at the earth's surface. *Am Meteorol Soc* 34:235–244
- Ferreira NJ, Correia AA, Ramirez MCV (2004) Synoptic scale features of the tropospheric circulation over tropical South America during the WETAMC TRMM/LBA experiment. *Atmosfera* 17(1):13–30
- Figueroa SN, Bonatti JP, Kubota PY, Grell GA, Morrison H, Barros SRM, Fernandez JPR, Ramirez E, Siqueira L, Luzia G, Silva J, Silva JR, Pendaharkar J, Capistrano VB, Alvim DS, Enoré DP, Diniz FLR, Satyamurty P, Cavalcanti IFA, Nobre P, Barbosa HMJ, Mendes CL, Panetta J (2016) The Brazilian global atmospheric model (BAM): performance for tropical rainfall forecasting and sensitivity to convective scheme and horizontal resolution. *Weather Forecast* 31:1547–1572
- Foss M (2011) Condições atmosféricas conducentes à ocorrência de tempestades convectivas severas na América do Sul. Dissertation, Federal University of Santa Maria
- Galway J (1956) The lifted index as a predictor of latent instability. *Bull Am Meteorol Soc* 37:528–529
- Gisini VA, Mote TL, Brooks HE (2014) Severe thunderstorm reanalysis environments and collocated radiosonde observations. *J Appl Meteorol Climatol* 53:742–751. <https://doi.org/10.1175/JAMC-D-13-0263.1>
- Gottlieb RJ (2009) Analysis of stability indices for severe thunderstorms in the northeastern United States. Dissertation, Cornell University
- Gulizia C, Camilloni I (2014) Comparative analysis of the ability of a set of CMIP3 and CMIP5 global climate models to represent precipitation in South America. *Int J Climatol* 35:583–595
- Haklander AJ, Van Delden A (2003) Thunderstorm predictors and their forecast skill for the Netherlands. *Atmos Res* 67–68:273–299
- Hart RE, Forbes GS, Grum RH (1998) The use of hourly model-generated soundings to forecast mesoscale phenomena. Part I: Initial assessment in forecasting warm-season phenomena. *Weather Forecasting* 13:1165–1185. [https://doi.org/10.1175/1520-0434\(1998\)013<1165:FTTUOH.2.0.CO;2](https://doi.org/10.1175/1520-0434(1998)013<1165:FTTUOH.2.0.CO;2)
- Holton JR, Pyle J, Curry JA (2002) Encyclopedia of Atmospheric Sciences. Academic Editor, New York,
- Huntrieser H, Schiesser H, Schmid W, Waldvogel A (1996) Comparison of traditional and newly developed thunderstorm indices for Switzerland. *Weather Forecast* 12:108–125
- Jacovides CP, Yonetani T (1990) An evaluation of stability indices for thunderstorm prediction in Greater Cyprus. *Weather Forecast* 5:559–569
- Jewell R, Brimelow J (2009) Evaluation of Alberta hail growth model using severe hail proximity soundings from the United States. *Weather Forecasting* 24:1592–1609
- Jones C, Carvalho LMV (2013) Climate change in the South American monsoon system: Present climate and CMIP5 projections. *J Clim* 26:6660–6678
- Kirkpatrick C, McCaul EW, Cohen C (2009) Variability of updraft and downdraft characteristics in a large parameter space study of diurnal convection *Mon Weather Rev* 10.1175/2008MWR2703.1
- Kottayil A, Buehler SA, John VO, Miloshevich LM, Milz M, Holl G (2001) On the importance of Vaisala RS92 radiosonde humidity corrections for a better agreement between measured and modeled satellite radiances. *Atmos Ocean Technol.* <https://doi.org/10.1175/JTECH-D-11-00080.1>

- Kunz M (2007) The skill of convective parameters and indices to predict isolated and severe thunderstorms. *Nat Hazards Earth Syst Sci* 7:327–342
- Li L, Gochis DJ, Sobolowski S, Mesquita MD (2017) Evaluating the present annual water budget of a Himalayan headwater river basin using a high-resolution atmosphere-hydrology model. *J Geophys Res Atmos* 122:4786–4807
- Lopez P (2007) Cloud and precipitation parameterizations in modeling and variational data assimilation: a review. *J Atmos Sci* 64:3766–3784
- Manzato A (2008) A Verification of Numerical Model Forecasts for Sounding-Derived Indices above Udine. NE Italy. *Weather Forecasting* 23(3):477–495
- Manzato A, Morgan G Jr (2003) Evaluating the sounding instability with the lifted parcel theory. *Atmos Res* 67–68:455–473
- Marinaki A, Spiliotopoulos M, Michalopoulou H (2006) Evaluation of atmospheric instability indices in Greece. *Adv Geosc* 7:131–135
- Markowski PM, Straka JM, Rasmussen EN (2002) Direct surface thermodynamic observations within the rear-flank downdrafts of nontornadoic and tornadoic supercells. *Mon Weather Rev* 130:1692–1721
- Mattioli V, Westwater ER, Cimmini D, Liljegren JC, Lesh BM, Gutman SI, Schmidlin FJ (2007) Analysis of radiosonde and ground-based remotely sensed PWV data from the 2004 North Slope of Alaska Arctic Winter Radiometric Experiment. *J Atmos Ocean Technol*. <https://doi.org/10.1175/JTECH1982.1>
- McCaul EW Jr, Cohen C (2002) The impact on simulated storm structure and intensity of variations in the mixed layer and moist layer depths. *Mon Weather Rev* 130:1722–1748
- Miglietta MM, Manzato A, Rotunno C (2016) Characteristics and Predictability of a Supercell during HyMeX SOP1: Characteristics and Predictability of a Supercell during HyMeX SOP1. *Q J R Meteorol Soc* 142:2839–2853
- Miller RC (1972) Notes on analysis and severe storm forecasting procedures of the Air Force GlobalWeather Center, AWS Tech. Report 200 (Rev.), Headquarters Air Weather Service, Scott AFB, pp 106
- JTS Moore, M Nolan, FH Glass, DL Ferry, SM Rochette (1995) Flash flood-producing high-precipitation supercells in Missouri. Preprints. In: 14th Conference on weather analysis and forecasting, Dallas, TX American Meteorological Society (J4), pp 7–12
- Nallapareddy A, Shapiro A, Gourley JJ (2011) A Climatology of nocturnal warming events associated with cold-frontal passages in Oklahoma. *J Appl Meteorol Clim* 50:2042–2061. <https://doi.org/10.1175/JAMC-D-11-020.1>
- Nascimento EL (2005) Previsão de tempestades severas utilizando-se parâmetros convectivos e modelos de mesoescala: uma estratégia operacional adotável no Brasil? *Rev Bras Meteorol* 20(1):113–122
- Ninomiya K (2007) Similarity and difference between the South Atlantic convergence zone and the Baiu frontal zone simulated by an AGCM. *J Meteorology Soc* 85:277–299
- Oakley NS, Lancaster JT, Kaplan ML, Ralph FM (2017) Synoptic conditions associated with cool season post-fire debris flows in the Transverse Ranges of southern California. *Nat Hazards*. <https://doi.org/10.1007/s11069-017-2867-6>
- Onderlinde MJ, Fuelberg HE (2014) A parameter for forecasting tornadoes associated with landfalling tropical cyclones. *Weather Forecasting* 29:1238–1255
- Pardo SK (2009) High-resolution analysis of the initiation of deep convection forced by boundary-layer processes. Dissertation, Karlsruhe University
- Púčik T, Groenemeijer P, Rýva D, Kolár M (2015) Proximity soundings of severe and nonsevere thunderstorms in central Europe. *Mon Weather Rev*. 143:4805–4821. <https://doi.org/10.1175/MWR-D-15-0104.1>
- Quadro MFL, Silva Dias MAFd, Herdies DL, Gonçalves LGG (2012) Análise climatológica da precipitação e do transporte de umidade na região da ZCAS através da nova geração de reanálises. *Rev Bras Meteorol* 27(2):152–162
- Ratnam MV, Santhi YD, Rajeevan M, Rao SVB (2013) Diurnal variability of stability indices observed using radiosonde observations over a tropical station: comparison with microwave radiometer measurements. *Atmos Res* 124:21–33
- Reid GC, Gage KS (1891) On the annual variation in height of the tropical tropopause. *J Atmos Sci*. 38:1928–1938
- Revathy K, Prabhakaran Nayar SR, Krishna Murthy BV (2001) Diurnal variation of tropospheric temperature at a tropical station. *Ann. Geophys.* 19:1001–1005
- Roe GH, Montgomery DR, Hallet B (2003) Orographic precipitation and the relief of mountain ranges. *J Geophys Res Solid Earth*. <https://doi.org/10.1029/2001JB001521>
- Satyamurti P, Rao VB (1988) Zona de Convergência do Atlântico Sul. *Climanálise* 3:31–35
- Schumacher R, Johnson RH (2005) Organization and environmental properties of extreme-rain-producing mesoscale convective systems. *Mon Wea Rev* 133:961–976
- Schumacher RS, Peters JM (2017) Near-surface thermodynamic sensitivities in simulated extreme-rain-producing mesoscale convective systems. *Mon Weather Rev* 145:2177–2200. <https://doi.org/10.1175/MWR-D-16-0255.1>
- Seidel DJ, Free M, Wang J (2005) Diurnal cycle of upper-air temperature estimated from radiosondes. *J Geophys Res*. <https://doi.org/10.1029/2004JD005526>
- Seluchi ME (2009) Chou ESC (2009) Synoptic patterns associated with landslide events in the Serra do Mar Brazil. *Theor Appl Clim*. 98:67–77
- Sherwood SC (2000) Climate signal mapping and an application to atmospheric tides. *Geophys Res Lett* 27:3525–3528
- Silva FP, Justi da Silva MGA, Menezes WF, Almeida VA (2016) Avaliação de indicadores atmosféricos utilizando o modelo numérico WRF em eventos de chuva na cidade do Rio de Janeiro. https://doi.org/10.11137/2015_2_81_90
- Silva FP, Justi-da-Silva MGA, Rotunno Filho OC, Pires GD, Sampaio RJ, Magalhães AAA (2018) Synoptic thermodynamic and dynamic patterns associated with Quitandinha River flooding events in Petropolis, Rio de Janeiro (Brazil) *Meteorol Atmos Phys* 25:25 doi: 10.1007/s00703-018-0609-2.
- Silva FP, Rotunno Filho OC, Sampaio RJ, Dragaud ICV, Magalhães AAA, Justi da Silva MGA, Pires GD (2017) Evaluation of atmospheric thermodynamics and dynamics during heavy-rainfall and no-rainfall events in the metropolitan area of Rio de Janeiro. *Brazil Meteorol Atmos Phys*. <https://doi.org/10.1007/s00703-017-0570-5>
- Silva Dias MAF (1987) Sistemas de mesoescala e previsão de tempo a curto prazo. *Rev Bras Meteorol* 2:133–150
- Silva Dias MAF (2000) Índices de instabilidade para previsão de chuva e tempestades severas. Departamento de Ciências Atmosféricas. https://www.redemet.aer.mil.br/uploads/2014/04/indice_sweat.pdf. Accessed date 02 March 2018
- Silvestro F, Rebora N, Cummings G, Ferraris L (2015) Experiences of dealing with flash floods using an ensemble hydrological nowcasting chain: implications of communication, accessibility and distribution of the results *J Flood Risk Manag* doi:10.1111/jfr3.1216 (in press)
- Tajbakhsh S, Ghafarian P, Sahraian F (2012) Instability indices and forecasting thunderstorms: the case of 30 April 2009. *Nat Hazards Earth Syst Sci* 12:1–11. <https://doi.org/10.5194/nhess-12-403-2012>
- Teixeira MS, Satyamurti P (2007) Dynamical and synoptic characteristics of heavy rainfall episodes in southern Brazil. *Mon. Weather Rev.* 135:598–617
- Trier SB, Davis CA, Ahijevych DA (2010) Environmental controls on the simulated diurnal cycle of warm-season precipitation in the

- continental United States. *J Atmos Sci* 67:1066–1090. <https://doi.org/10.1175/2009JAS3247.1>
- Tuttle JD, Davis CA (2006) Corridors of warm season precipitation in the central United States. *Mon Weather Rev.* 134:2297–2317. <https://doi.org/10.1175/MWR3188.1>
- Wagner TH, Feltz WF, Ackerman SA (2008W) The Temporal evolution of convective indices in storm-producing environments. *Weather Forecast* 23:786–794. <https://doi.org/10.1175/2008WAF2007046.1>
- Weisman M, Klemp JB (1982) The dependence of numerically-simulated diurnal convection on vertical wind shear and buoyancy. *Mon Weather Rev* 110:504–520
- Weisman ML, Klemp JB (1986) Characteristics of Isolated Diurnal convection. Ray PS *Mesoscale Meteorology and Forecasting*. American Meteorological Society, Boston, pp 331–358
- Westwater ER, Boba Stankov B, Cimini D, Han Y, Joseph A, Lesht BM, Long CN (2003) Radiosonde humidity soundings and microwave radiometers during Nauru99. *J Atmos Ocean Technol.* 20:953–971
- Wetzel SW, Martin JE (2001) An Operational Parameters – Based Methodology For Forecasting Midlatitude Winter Season Precipitation. *Weather Forecast* 16:156–167
- Wilde NP, Stull RB, Eloranta EW (1985) The LCL zone and cumulus onset. *J. Clim Appl Meteorol* 24:640–657. [https://doi.org/10.1175/1520-0450\(1985\)024,0640:TLZACO.2.0.CO;2](https://doi.org/10.1175/1520-0450(1985)024<0640:TLZACO.2.0.CO;2)
- WMO (2018) World Meteorological Organization. https://library.wmo.int/opac/doc_num.php?explnum_id=3795. Accessed 02 March 2018
- Wyszogrodzki AA, Liu Y, Jacobs N, Childs P, Zhang Y, Roux G, Warner TT (2013) Analysis of the surface temperature and wind forecast errors of the NCAR-AirDat operational CONUS 4-km WRF forecasting system. *Meteorol Atmos. Phys.* 122:125–143

Publisher's Note Springer Nature remains neutral with regard to jurisdictional claims in published maps and institutional affiliations.